"Layering" effect in a sheared lyotropic lamellar phase

O. Diat,*,† D. Roux, and F. Nallet
Centre de recherche Paul-Pascal, CNRS, Avenue du Docteur-Schweitzer, F-33600 Pessac, France
(Received 20 September 1994)

In certain cases, lyotropic lamellar phases under shear form structures corresponding to a close-packed assembly of multilayered vehicles. We present light and neutron scattering data showing that these micrometer-sized objects may exhibit a long-range order under shear similar to that which has been observed for rigid colloidal particles (shear-induced ordering).

PACS number(s): 82.70.−y, 61.30.Gd, 83.70.Jr

INTRODUCTION

Lyotropic lamellar phases are liquid crystalline phases (smectic *A*) sometimes obtained when surfactant molecules are dissolved in organic or aqueous solvents [1]. These phases are made of regularly stacked planar *membranes* (surfactant bilayers, with a thickness δ a few nanometers and of infinite lateral extent), separated by solvent. Depending on the physico-chemical nature of the system (determined by the choice of surfactants, cosurfactants, and solvents) the long-range positional order may still exist at high dilution (low surfactant content) leading to a smectic period d sometimes as large as about 1 μm [2–4]. This property is often attributed to the long-range repulsive interaction between membranes that arises from the steric hindrance to membrane undulations [5,6].

A lot of information on the *equilibrium* static or dynamic behavior of such systems has been gained from the intense interest in the thermodynamic stability and elastic properties of these multilayered systems [5–14]. *Out-of-equilibrium* studies are less abundant, however; recently we started to investigate the effect of a shear flow on lyotropic lamellar phases [15,16]. More specifically, we connected the orientation steady states that obtain under shear to the theological behavior of a lamellar phase [17].

This paper is organized as follows. First, we recall previous results on the orientation diagram of sheared lamellar phases. Second, we describe a shear-ordering ("layering") effect observed in the studied sample. It corresponds to a two-dimensional kind of crystallization of the so-called spherulite structure. Finally, we analyze our data with a simple model and present some experimental perspectives.

ORIENTATION DIAGRAM

The orientation diagram, which describes steady states of well-defined orientations (together with the out-of-equilibrium transitions between them) as a function of shear, was established in cylindrical Couette cells. In our setup, the inner cylinder is fixed. When the outer cylinder rotates at constant speed an average tangential flow obtains with a radial gradient, corresponding to a shear flow. More detailed information on the design of the cells (temperature regulated; transparent to both neutron radiation and light) may be found in another paper [16].

In the case previously studied in detail (an inverse lamellar phase with sodium dodecylsulphate-pentanol bilayers, slightly swollen by water and separated by variable amounts of dodecane) three steady states are observed [16]. At low shear rates there is a state (state I) that consists of a *partially oriented* lamellar phase; the membranes are stacked mainly along the radial direction and therefore laid parallel to the surfaces of the cylinders; many defects are still present that probably move along the flow. At high shear rates a somewhat similar state (state III) is observed. Its main difference with state I is that it is much better oriented; membranes stacked along the tangential (flow) direction are no longer present, while there are still some defects with membranes stacked parallel to the symmetry axis. Between states I and III, at intermediate shear rates a striking organization for the membranes is observed: in state II, the membranes are wrapped in multilamellar vesicles (or *spherulites),* apparently close packed. The size of these spherulites depends on the shear rate, decreasing from typically 10 μm to less than 1 μm as shear increases [15]. Besides, it was noticed that the smectic period remained constant whatever the shear rate. States I and II have also been observed with several other lyotropic lamellar systems [18].

As shown previously [16], state II can be characterized using scattering techniques (with usually radially incident radiations); the neutron scattering spectrum is that of a perfect powder, meaning that the local stacking direction is evenly distributed in space; light scattering yields an isotropic ring at a finite wave vector from which a glass-like organization of objects with a well-defined size is in-

*Present address: Installation Européenne de Rayonnement Synchrotron, ESRF, Boîte Postale 220, F-38043 Grenoble, France.
†Author to whom correspondence should be addressed. Tel: +33 76 88 21 21; Electronic address: diat@esrf.fr

ferred. In what follows we present scattering data for a lamellar system showing that beyond states I and II a new state of orientation may be found instead of (or before) state III. In this new state the spherulites that are close packed at random in state II get *long-range ordered* in two-dimensional layers with hexagonal symmetry perpendicular to the radial directions. The positional long-range order of the spherulites is associated to an *orientational* order to the membrane stacking directions. This reveals that in this state the spherulites are objects with a six-fold symmetry around the radial axis.

SHEAR ORDERING

The system we consider here is prepared with sodium dodecylsulphate (SDS), octanol, and water salted with 20 g/l of sodium chloride. An account of the phase diagram may be found elsewhere [19]. The lamellar phase can be described as SDS-octanol membranes separated by water. Previous experimental work demonstrated that entropically driven undulation forces stabilize this system in the dilute limit [20] (the electrostatic interaction between charged membranes is screened out in the salted solvent). In the present study, the membrane (i.e., SDS + octanol) volume fraction is about 19%, with a SDS-pentanol mass ratio 0.9; the smectic period, as determined by neutron scattering [21] (on a sample where water is replaced by D_2O; this affects negligibly the phase boundaries) is $d = 11.4$ nm. Figure 1 shows schematically the geometry of the setup for the small-angle scattering experiments; neutron or light beams go through the Couette cell along the radial direction; access to the reciprocal space is thus provided with wave vectors within the symmetry axis–tangential axis plane.

With this system, we observe states I and II in a range of shear rates comparable to previous results [16]. Below about 1 s^{-1} the orientational state is macroscopically steady and corresponds to state I. Neutron scattering shows that membranes are mainly parallel to the cylindrical boundaries, with many defects. There are no remarkable features in light scattering, apart from a very small

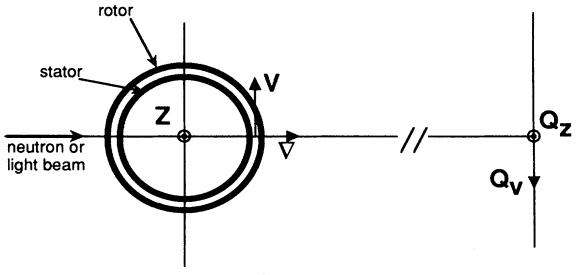

FIG. 1. Schematic setup for the light and small-angle neutron scattering measurements, with the principal axes. The (laser light or neutron) beam goes through the cell along the radial (velocity gradient ∇) direction. The vertical axis, denoted **Z**, is parallel to the Couette cell symmetry (rotation) axis. The average flow is along the tangential axis **V**. The detector (a screen, or a 128×128 square multidetector) is in the symmetry axis–tangential axis plane, with principal wave vectors denoted $\mathbf{Q}_Z$ and $\mathbf{Q}_V$.

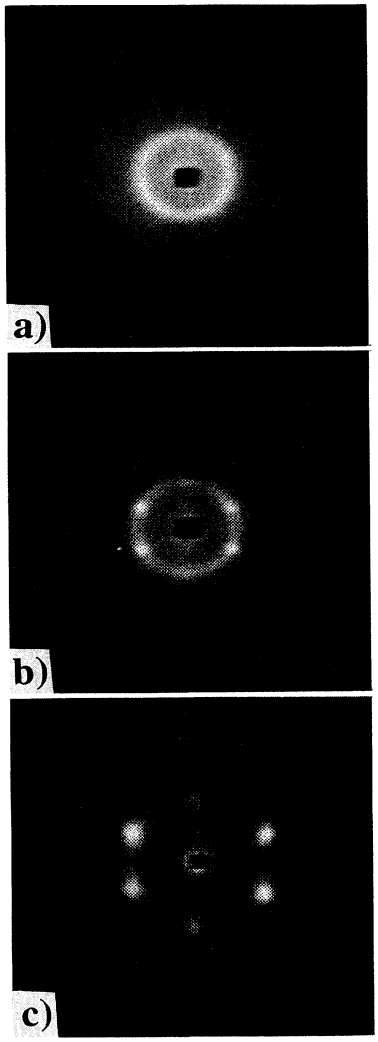

FIG. 2. Evolution of the light scattering pattern with shear rate [(a) $\dot{\gamma} = 1$ s^{-1}; (b) $\dot{\gamma} = 9.9$ s^{-1}; (c) $\dot{\gamma} = 1070$ s^{-1}].

angle signal around the beam stop. Just above 1 s^{-1}, a well-defined *isotropic* diffraction ring is observed with light scattering [Fig. 2(a)], associated with an *isotropic* Bragg ring in neutron scattering [Fig. 3(a)]. These features reveal the spherulite state of orientation (state II), confirmed by an observation under microscope [22]. The spherulites are close packed, with a size about 5 μm. When shear is increased above 7 s^{-1}, the evolution differs from the one described previously [16]; instead of observing in light scattering a ring with increasing diameter that eventually disappears upon entering state III, we get superimposed on the ring six well-defined and intense spots [see Fig. 2(b)]. As shear increases, the diameter of the ring remains constant and the six spots become comparatively more intense. At the highest available shear rates (typically 1000 s^{-1}), the ring is no longer seen [Fig. 2(c)]. Note that the spots with wave vectors *along* the

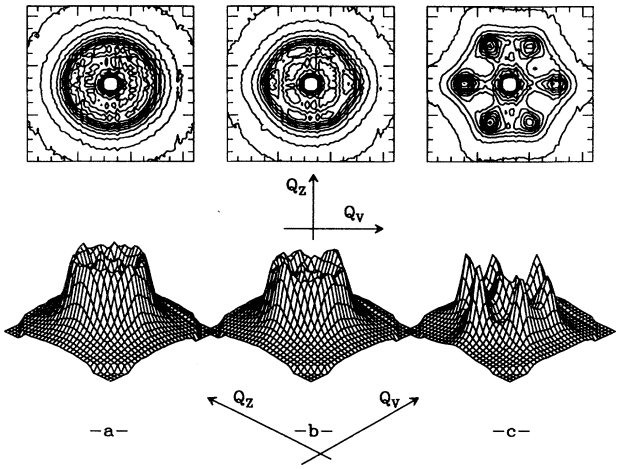

FIG. 3. Evolution of the small-angle neutron scattering pattern with shear rate [(a) = 1.3 s^{-1}; (b) $\dot{\gamma}=9.9\ s^{-1}$; (c) $\dot{\gamma}=780\ s^{-1}$].

Couette cell symmetry axis are less intense than the other four spots [Figs. 2(b) and 2(c)].

Figure 3 displays the evolution of the small-angle neutron scattering signal; at shear rate 1.3 s^{-1} [Fig. 3(a)], the pattern is isotropic with Bragg scattering on a ring, as mentioned above. The Bragg peak is located at $q_0=0.55$ nm^{-1}. The same scattering pattern (and the same q_0) is observed when the Couette cell is sharply brought to rest. Figure 3(b) shows the pattern at 9.9 s^{-1}; the Bragg intensity is modulated along the azimuthal angle, with six humps appearing, separated by approximately $\pi/3$ rad. Then, at higher shear rates, we observe the splitting of the Bragg ring into six well-defined peaks [Fig. 3(c), corresponding to 780 s^{-1}].

Another interesting phenomenon appears as the hexagonal pattern forms; there is a shift in the Bragg peak position. As shown in Fig. 4, the Bragg wave vector first increases with shear and then reaches apparently a plateau in the range investigated. This suggests that water is expelled from the intermembranar space, leading to a reduced smectic period. Note also that the hexagonal patterns observed in both neutron and light scattering at high shear rates are rotated with respect to each other by

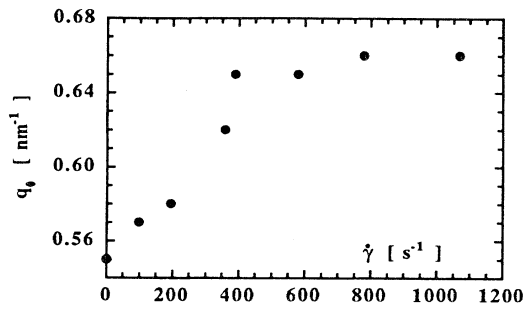

FIG. 4. Variation of the Bragg peak position q_0 versus shear rate.

$\pi/6$ rad; one finds two vertices along the Couette cell symmetry axis in light scattering [Figs. 2(b) and 2(c)] and two vertices along the tangential direction in neutron scattering [Figs. 3(b) and 3(c)].

ANALYSIS

The diffraction patterns observed with small-angle neutron and light scattering at different length scales (a few micrometers with light; a few tens of nanometers with neutrons) may be interpreted with the following schematic picture (Fig. 5): at high shear rates, there is an *orientational* order with a sixfold symmetry of the membrane stacking directions in the symmetry axis–tangential axis plane of the Couette cell. That order arises because hexagonal-shaped spherulites, all of the same size, are close packed with long-range *positional* order on parallel triangular lattices; one then expects diffraction patterns from the layered structure (neutron scale) and from the two-dimensional-crystalline structure (light scale) to be rotated with respect to each other by $\pi/6$ rad, as actually observed. At lower shear rates, state II is *locally* presumably quite similar, with the difference being that the above-described orientational and positional orders have in this case a finite range only; the peaks and spots are blurred by macroscopic disorder and become rings. In the long-range-ordered state, some water is locally expelled from the lamellar systems; it might be located between adjacent regions with hexagonal arrangement, sliding over each other. This type of shear ordering would then be similar to the one already observed in colloidal suspensions of hard spheres and called a layering effect [23,24]. In such systems, consecutive regions with hexagonal order slide over each other with zig-zag motions away from the average flow direction. The same kind of motions might occur with our system; this could explain the two less well-defined spots we observe in light scattering [25].

In our previous study, the *size* of the spherulites in state II was predicted, as a function of shear with a rath-

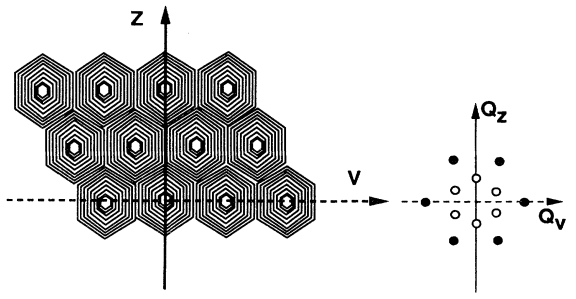

FIG. 5. Schematic organization of the spherulites in real space (left drawing) and in reciprocal space (right drawing), at high shear rates. The neutron, large wave vector spots (●) are related to the period d of the layered membrane structure and located at $q_0=2\pi/d$. The light, small wave vector spots (○) are related to the spherulite structure and located at $2\pi/D$, with D the spherulite size. The structure is locally the same in state II, with local crystallographic axes disordered with respect to **Z** and **V** axes.

er simple argument [16]. The bending energy of a multilamellar vehicle (described as a sphere of radius R),

$$E_b = 4\pi(2\kappa+\bar{\kappa})\frac{R}{d} , \quad (1)$$

where κ and $\bar{\kappa}$ are the mean and Gaussian curvature moduli, respectively [26], is balanced against the Taylor estimate of the energy in the viscous flow [27]:

$$E_v = \eta\dot{\gamma}R^3 , \quad (2)$$

where η is the viscosity and $\dot{\gamma}$ the (average) shear flow. This yields the $R \sim \dot{\gamma}^{-1/2}$ scaling law experimentally observed.

In the present case, the size of the spherulites no longer varies with shear once the "layering" effect appears. One may then wonder what happens with the unbalanced viscous term in the previous equation. We propose here that it is used to reduce the spacing of the layered structure, leading to an increase in the Bragg wave vector (Fig. 4). Writing the argument as

$$\tfrac{2}{3}\pi R^3 \bar{B}\left[\frac{\Delta d}{d}\right]^2 + 4\pi(2\kappa+\bar{\kappa})\frac{R}{d} = \eta\dot{\gamma}R^3 , \quad (3)$$

where now a layer compression term (with $\bar{B}$ the layer compression modulus) is added to the bending term [Eq. (1)], we get (estimating the smectic compression modulus $\bar{B} \approx 103$ Pa [20] and with a viscosity $\eta \approx 10^{-2}$ Pa/s) a $\Delta d/d \approx 7\%$ relative variation of the period d at $\dot{\gamma} = 1000$ s^{-1}. This is rather compatible with the experimental observation and suggests that the shear stress that was used to fix the size of the spherulites is indeed used in the shear-ordered state to reduce the smectic spacing.

CONCLUSION

In this study, we show a new feature in the orientation diagram of a sheared lamellar phase, namely a shear ordering or layering effect. We find the previously observed [16] isotropic, glasslike spherulite organization of the lamellar phase at low shear rates but this steady orientational state is not followed as shear is increased (for the pseudoternary system we investigate here) by the oriented state. Instead, we observe at higher shear rates that spherulites stop changing their size and organize themselves into long-range-ordered plane structures sliding over each other. In these ordered structures the spherulites are hexagonal shaped and close packed on triangular lattices. The shear ordering is accompanied by a decrease in the smectic period.

ACKNOWLEDGMENTS

The authors would like to thank Annie Brûlet and Laurence Noirez for their helpful assistance at Laboratoire Léon-Brillouin. They also thank Noel Clark for his many pertinent advices.

[1] P. Ekwall, in *Advances in Liquid Crystals,* edited by G. M. Brown (Academic, New York, 1975).
[2] A.-M. Bellocq and D. Roux, in *Microemulsion,* edited by S. Friberg and P. Bothorel (CRC Press, Boca Raton, FL, 1986).
[3] F. C. Larche, J. Appell, G. Porte, P. Bassereau, and J. Marigan, Phys Rev. Lett. **56**, 1700 (1986).
[4] F. Lichterfeld, T. Schmeling, and R. Strey, J. Phys. Chem. **90**, 5762 (1986).
[5] W. Helfrich, Z. Naturforsch Teil A **33**, 305 (1978).
[6] D. Roux and C. R. Safinya, J. Phys. (France) **49**, 307 (1988); C. R. Safinya, D. Roux, G. S. K. Smith, S. K. Sinha, P. Dimon, N. A. Clark, and A.-M. Bellocq, Phys. Rev. Lett. **57**, 2718 (1986).
[7] P.-G. de Gennes, J. Phys. Suppl. **30**, C4-65 (1969).
[8] A. Caille, C. R. Acad. Sci. B **274**, 891 (1972).
[9] F. Brochard and P.-G. de Gennes, Pramana Suppl. **1**, 1 (1975).
[10] M. Kleman, in *Points Lignes Parois* (Editions de Physique CNRS, Paris, 1977).
[11] W. Helfrich and R. M. Servusso, Nuovo Cimento **3**, 137 (1984).
[12] F. Nallet, D. Roux, and J. Prost, J. Phys. (France) **50**, 3147 (1989).
[13] R. Strey, R. Schomäker, D. Roux, F. Nallet, and U. Olsson, J. Chem. Soc. Faraday Trans. **86**, 2253 (1990).
[14] D. Roux, C. R. Safinya, and F. Nallet, in *Micelles, Membranes, Microemulsions and Monolayers,* edited by W. Gelbart, A. Ben Shaul, and D. Roux (Springer-Verlag, New York, 1994).
[15] O. Diat and D. Roux, J. Phys. (II) France **3**, 9 (1993).
[16] O. Diat, D. Roux, and F. Nallet, J. Phys. (II) France **3**, 1427 (1993); O. Diat, Ph.D. thesis, Université Bordeaux-I, France (1992).
[17] D. Roux, F. Nallet, and O. Diat, Europhys. Lett. **24**, 53 (1993).
[18] Different systems include nonionic and ionic surfactants in brine; direct and inverted bilayers; D. Roux and O. Diat, French Patent No. 9204108.
[19] P. Herve, D. Roux, A.-M. Bellocq, F. Nallet, and T. Gulik-Krzywicki, J. Phys. (II) France **3**, 1255 (1993).
[20] F. Nallet and D. Roux (unpublished).
[21] The neutron scattering experiments are made on the beam line PAXY at Laboratoire Léon-Brillouin, laboratoire commun CEA/CNRS.
[22] The observation in real space is possible using a special home-made plane-plane shear cell located under a polarizing microscope and also with freeze-fracture electron microscopy; P. Sierro and D. Roux (unpublished).
[23] B.J. Ackerson and N. A. Clark, Phys. Rev. A **30**, 906 (1984).
[24] M. Tomita and T. G. M. van de Ven, J. Colloid Interface Sci. **99**, 374 (1984).
[25] N. A. Clark (private communication).
[26] W. Helfrich, Z. Naturforsch. Teil C **28**, 695 (1973).
[27] G. I. Taylor, Proc. R. Soc. London Ser. A **138**, 41 (1932); **146**, 501 (1934).

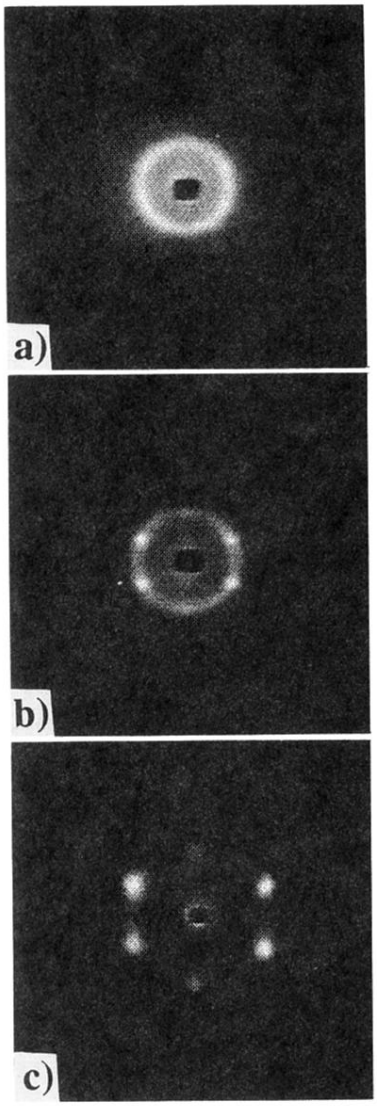

FIG. 2. Evolution of the light scattering pattern with shear rate [(a) $\dot{\gamma}=1\ s^{-1}$; (b) $\dot{\gamma}=9.9\ s^{-1}$; (c) $\dot{\gamma}=1070\ s^{-1}$].